

2
3
4
5
6
7
8
9
10
11
12
13
14
15
16
17
18
19

Identification of Adomavirus Virion Proteins

Nicole L. Welch¹, Michael J. Tisza¹, Gabriel J. Starrett¹, Anna K. Belford¹, Diana V. Pastrana¹,
Yuk-Ying S. Pang¹, John T. Schiller¹, Ping An², Paul G. Cantalupo², James M. Pipas², Samantha
Koda³, Kuttichantran Subramaniam³, Thomas B. Waltzek³, Chao Bian⁴, Qiong Shi⁴, Zhiqiang
Ruan⁴, Terry Fei Fan Ng⁵, and Christopher B. Buck^{1*}

¹Lab of Cellular Oncology, NCI, NIH, Bethesda, MD, 20892 USA

²Dept. of Biological Sciences, Univ. of Pittsburgh, Pittsburgh, PA 15260 USA

³Dept. of Infectious Disease and Pathology, Univ. of Florida, Gainesville, FL, 32611 USA

⁴Shenzhen Key Lab of Marine Genomics, Guangdong Provincial Key Lab of Molecular Breeding
in Marine Economic Animals, BGI Academy of Marine Sciences, BGI, Shenzhen, Guangdong
518083, China

⁵College of Veterinary Medicine, University of Georgia, Athens, GA 30602 USA

*Corresponding author: buckc@mail.nih.gov

20

21

Abstract

22 Adenoviruses, papillomaviruses, and polyomaviruses are collectively known as small DNA
23 tumor viruses. Although it has long been recognized that small DNA tumor virus oncoproteins
24 and capsid proteins show a variety of structural and functional similarities, it is unclear whether
25 these similarities reflect descent from a common ancestor, convergent evolution, horizontal gene
26 transfer among virus lineages, or acquisition of genes from host cells. Here, we report the
27 discovery of a dozen new members of an emerging virus family, the *Adomaviridae*, that unite a
28 papillomavirus/polyomavirus-like replicase gene with an adenovirus-like virion maturational
29 protease. Adomaviruses were initially discovered in a lethal disease outbreak among endangered
30 Japanese eels. New adomavirus genomes were found in additional commercially important fish
31 species, such as tilapia, as well as in reptiles. The search for adomavirus sequences also revealed
32 an additional candidate virus family, which we refer to as xenomaviruses, in mollusk datasets.
33 Analysis of native adomavirus virions and expression of recombinant proteins showed that the
34 virion structural proteins of adomaviruses are homologous to those of both adenoviruses and
35 another emerging animal virus family called adintoviruses. The results pave the way toward
36 development of vaccines against adomaviruses and suggest a framework that ties small DNA
37 tumor viruses into a shared evolutionary history.

38

39

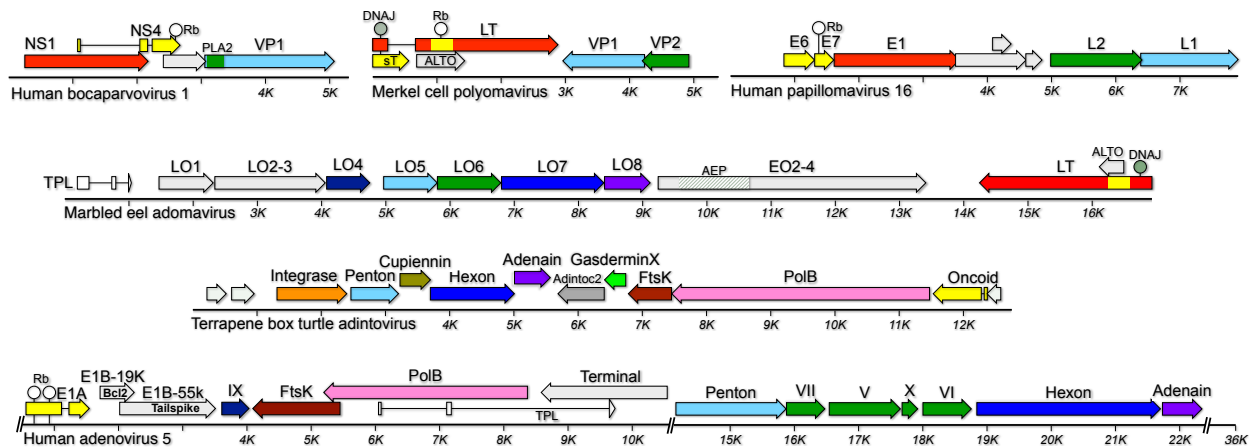
Author Summary

40 In contrast to cellular organisms, viruses do not encode any universally conserved genes. Even
41 within a given family of viruses, the amino acid sequences encoded by homologous genes can
42 diverge to the point of unrecognizability. Although members of an emerging virus family, the
43 *Adomaviridae*, encode replicative DNA helicase proteins that are recognizably similar to those of
44 polyomaviruses and papillomaviruses, the functions of other adomavirus genes have been
45 difficult to identify. Using a combination of laboratory and bioinformatic approaches, we
46 identify the adomavirus virion structural proteins. The results link adomavirus virion protein
47 operons to those of other midsize non-enveloped DNA viruses, including adenoviruses and
48 adintoviruses.

49

Introduction

50 Polyomaviruses, papillomaviruses, and adenoviruses are historically defined as small DNA
 51 tumor viruses (Pipas 2019). Although members of a fourth animal-tropic non-enveloped DNA
 52 virus family, the *Parvoviridae*, are not known to cause tumors they share a number of biological
 53 features with traditional small DNA tumor viruses. Each of the four virus families encodes non-
 54 enveloped virion proteins with similar pentameric single- β -jellyroll core folds and members of
 55 each of the four families express functionally similar oncogenes that inactivate cellular tumor
 56 suppressor proteins (Figure 1)(de Souza, Iyer et al. 2010, Krupovic and Koonin 2017). An
 57 emerging group of animal viruses called adintoviruses appears to represent a candidate fifth
 58 family with similarities to small DNA tumor viruses
 59 <https://www.biorxiv.org/content/10.1101/697771v3>.



60

61 **Figure 1: Maps of representative virus genomes.** Genes are color-coded based on
 62 known or inferred functions. Polyomaviruses, papillomaviruses, and adenoviruses have
 63 circular double-stranded DNA genomes that were linearized for display. Parvoviruses
 64 have linear single-stranded DNA (ssDNA) genomes, while adintoviruses and adenoviruses
 65 have linear dsDNA genomes. Symbols and abbreviations: white lollipop,
 66 retinoblastoma/pocket protein (Rb) interaction motif; gray lollipop, domain with predicted
 67 fold similar to DNAJ chaperone proteins; AEP, domain resembling archaeal-eukaryotic
 68 primase small catalytic subunit; PLA2, domain with predicted fold similar to
 69 phospholipase A2. See main text for other gene names.

70 Polyomaviruses, papillomaviruses, and parvoviruses are proposed to have descended from
 71 circular Rep-encoding single-stranded DNA (CRESS) virus ancestors (Koonin, Dolja et al.
 72 2015). This model explains the phylogenetic relationships of the replicative superfamily 3
 73 helicase (S3H) and rolling circle “nickase” endonuclease domain of CRESS virus and small
 74 DNA tumor virus replicase genes (Kazlauskas, Varsani et al. 2019), but it does not account for
 75 possible similarities between the virion proteins and accessory genes of the “-oma” families and
 76 adenoviruses. Achieving a better understanding of the relationships between small DNA tumor
 77 virus families has the potential to guide comparative studies of these common human pathogens.

78 In 2011, a previously unknown circular dsDNA virus was discovered in a lethal disease outbreak
 79 among Japanese eels (*Anguilla japonica*)(Mizutani, Sayama et al. 2011, Okazaki, Yasumoto et
 80 al. 2016). Two related viruses have since been isolated from Taiwanese marbled eels (*Anguilla*

81 *marmorata*) and a giant guitarfish (*Rhynchobatus djiddensis*)(Wen, Chen et al. 2015, Dill,
82 Camus et al. 2018). In contrast to the eel viruses, which encode S3H replicase proteins that
83 closely resemble the large tumor antigens (LT) of fish polyomaviruses, the guitarfish virus
84 encodes a distinct S3H replicase, called EO1, that is distant from LT and is instead more closely
85 related to the E1 replicases of papillomaviruses. The name “adomaviruses” has been applied to
86 this emerging family, connoting the fact that the three known species each encode homologs of
87 the adenain virion-maturational proteases of *adenoviruses* as well as *polyomavirus* and
88 *papillomavirus* S3H homologs.

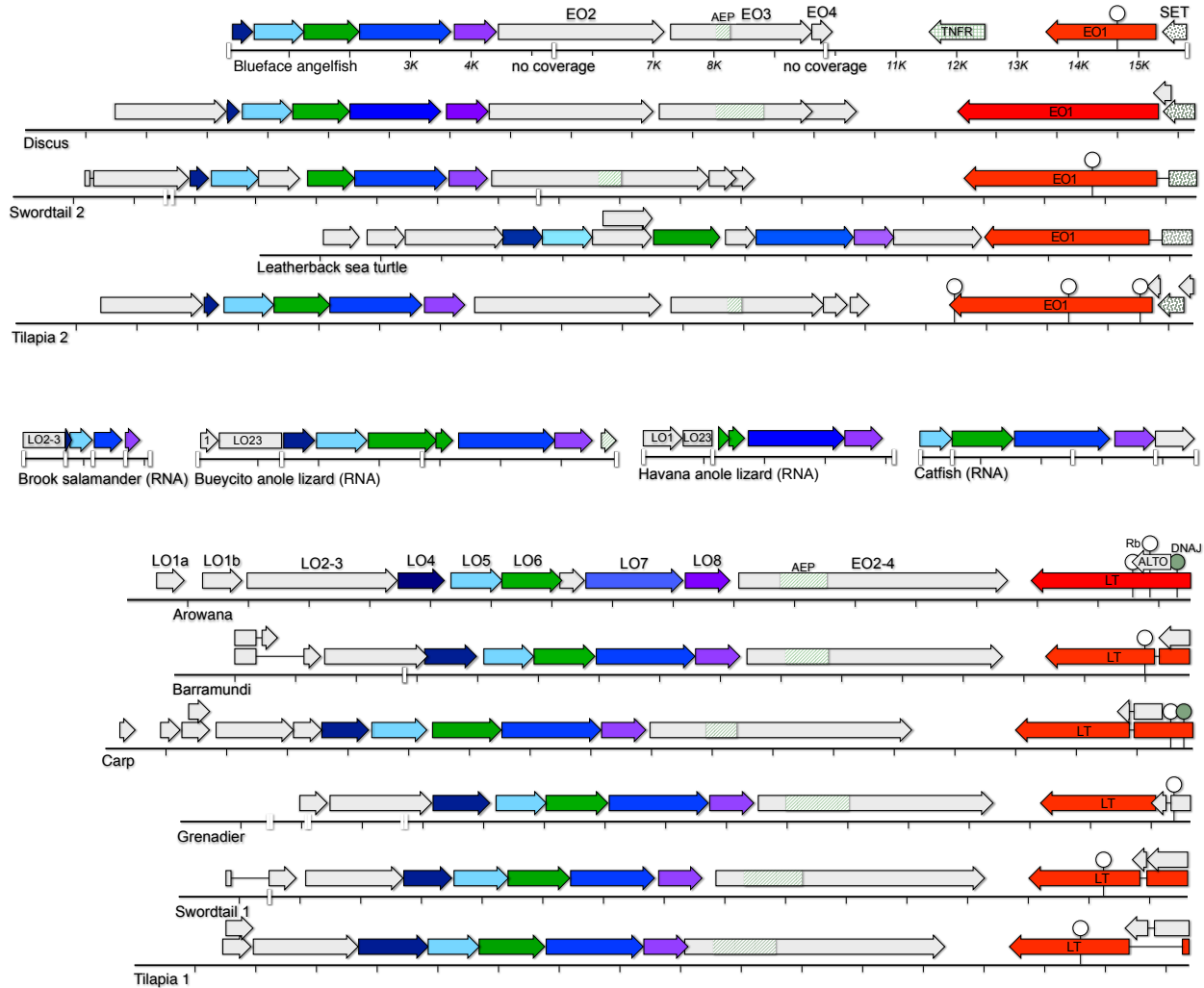
89 The primary goal of this study is to identify the adomavirus virion proteins and to uncover
90 possible evolutionary relationships to the virion proteins of small DNA tumor viruses. To
91 discover additional adomavirus species, we conducted metagenomic sequencing studies and
92 developed a pipeline to detect small DNA tumor virus-related sequences in the NCBI Sequence
93 Read Archive (SRA). Bioinformatic methods were used to predict which adomavirus ORFs
94 might represent virion proteins and the predictions were confirmed through functional expression
95 in cell culture. The results pave the way toward development of preventive vaccines against
96 pathogenic adomaviruses.

97

98 **Results**

99 **Detection of additional adomaviruses**

100 A post-mortem metagenomics analysis of an aquarium-bred Amazon red discus cichlid
101 (*Symphysodon discus*) exhibiting lethargy and inflamed skin lesions revealed a complete circular
102 adomavirus genome (Figure 2). Histopathological analysis of skin lesions from the discus
103 specimen showed no evidence of intranuclear inclusions or other obvious histopathology.



104

105 **Figure 2: Genome maps of previously unknown adomaviruses.** Genes were named
 106 based on conventions originally developed for Japanese eel adomavirus (NC_015123).
 107 Alpha adomaviruses (top half of figure) are defined by the presence of an adomavirus-
 108 specific S3H replicase, designated EO1. A row of fragmentary adomavirus sequences from
 109 RNA datasets are shown in the middle of the figure. Beta adomaviruses (bottom half of
 110 figure) encode a polyomavirus-like large tumor antigen (LT). In some cases, repetitive or
 111 GC-rich patches (particularly near the 3' end of the LO2-3 ORF) could not be resolved
 112 using available short-read datasets. Coverage gaps are represented as white bars on the
 113 ruler. A poorly conserved set of accessory genes upstream of Alpha adomavirus EO1 genes
 114 show varying degrees of similarity to the S-adenosyl methionine-binding pocket of cellular
 115 SET proteins, which function as histone lysine-methyltransferases. Adomavirus SET
 116 homologs are highly divergent from all previously described eukaryotic and viral SET
 117 genes. The same is true for adomavirus EO2-4 and EO3 segments that encode homologs of
 118 the catalytic small subunit of archaeal eukaryotic primases (AEPs, hatched boxes).

119 Figure supplement 1: a table of accession numbers and Linnaean designations of hosts

120 Figure supplement 2: examples of the annotation process

121 Figure supplement 3: GenBank-format nucleotide maps of adomaviruses

122 Figure supplement 4: protein compilations in fasta format

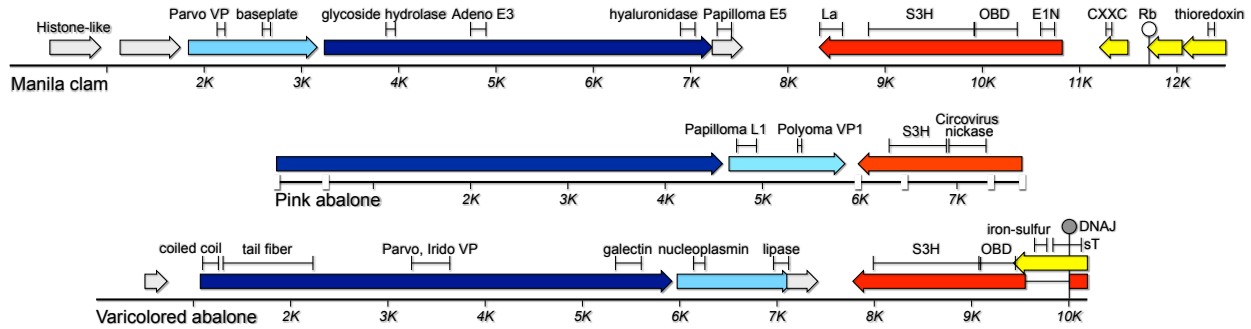
123 Figure supplement 5: splicing of marbled eel adomavirus transcripts

124 An adomavirus from an apparently healthy green arowana (*Scleropages formosus*) was first
125 identified in TBLASTN searches of the NCBI Whole-Genome Shotgun (WGS) database as a set
126 of short contigs with similarity to Japanese eel adomavirus proteins. A complete adomavirus
127 genome was characterized by Sanger sequencing of overlapping PCR products using DNA left
128 over from the original fin snip used for the WGS project (Bian, Hu et al. 2016).

129 The WGS TBLASTN survey also revealed a 4 kb contig with a sequence resembling adomavirus
130 LT in a dataset for western softhead grenadier fish (*Malacocephalus occidentalis*) and a nearly
131 complete adomavirus genome in a dataset for a skin biopsy of a leatherback sea turtle
132 (*Dermochelys coriacea*). Genome sequences for the two viruses were completed using parent
133 SRA datasets.

134 A pipeline using DIAMOND (a faster alternative to BLASTX (Buchfink, Xie et al. 2015)) was
135 developed to screen SRA datasets for fish, amphibians, and reptiles. SRA datasets rich in reads
136 encoding adomavirus-like protein sequences were subjected to *de novo* assembly. This approach
137 resulted in the identification of seven additional adomavirus genomes (Figure 2). Notably,
138 adomavirus sequences were found in genome sequencing datasets for farmed tilapia
139 (*Oreochromis niloticus*), which represent a \$7.5 billion per year global aquaculture industry, and
140 in the most extensively aquacultured fish in developing countries, the mirror carp (*Cyprinus*
141 *carpio*) (Bacharach, Mishra et al. 2016, Belton, Little et al. 2018). Adomavirus-like fragments
142 were also detected in transcriptomic datasets for brook salamander (*Calotriton asper*) and two
143 closely related species of anole lizard (genus *Anolis*).

144 The WGS search for adomavirus-like S3H sequences also led to the discovery of a divergent
145 class of circular DNA elements that we tentatively designate “xenomaviruses,” connoting the
146 exotic nature of their predicted S3H and virion proteins (Figure 2 Figure supplement 2, Figure 3,
147 and Figure 4). Intriguingly, a conserved xenomavirus ORF shows distant predicted structural
148 similarity to the L1 and VP1 penton proteins of papillomaviruses and polyomaviruses. The
149 inferred replicase gene of a partial xenomavirus sequence detected in a dataset for pink abalone
150 (*Haliotis corrugata*) encodes a domain with predicted structural similarity to the nickase domain
151 of porcine circovirus 2 (a CRESS virus). The identification of additional viruses in this class
152 could shed light on the evolutionary interrelationships between small DNA tumor viruses and
153 CRESS viruses.



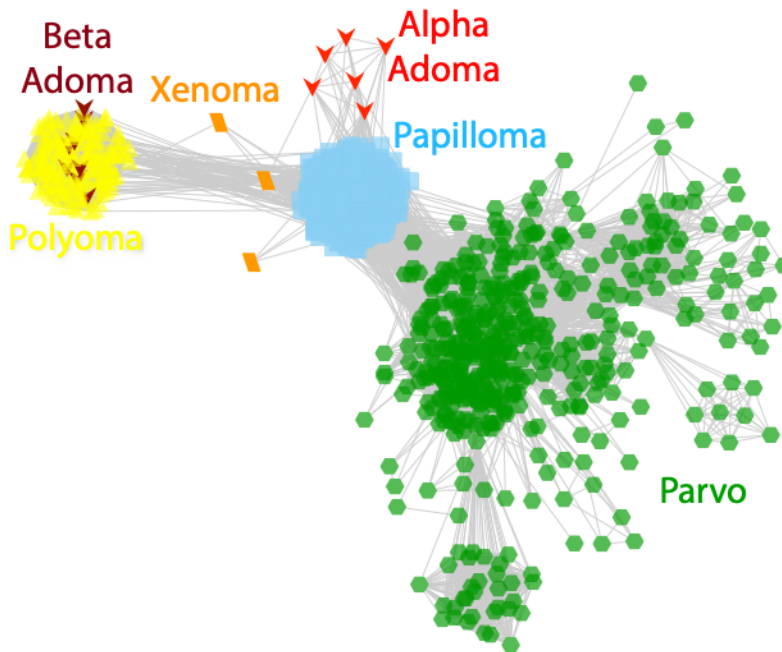
154

155 **Figure 3: Genome maps of candidate xenomaviruses.** Brackets indicate segments where
 156 remote similarities were detected in DELTA-BLAST, HHpred, and Phyre² searches. The
 157 functions of these segments remain hypothetical.

158

159 Adomavirus phylogeny

160 Adomavirus sequences can be divided into two groups based on their replicative S3H genes. A
 161 group we designate Alpha is defined by the presence of an EO1 S3H replicase gene that yields
 162 moderate hits (BLASTP E-values $\sim 1e-9$) for papillomavirus E1 proteins. Adomavirus group Beta
 163 is defined by the presence of an S3H replicase similar (E-values $\sim 1e-60$) to the LT proteins of
 164 polyomaviruses. A network display of BLASTP relationships is shown in Figure 4. The Alpha
 165 and Beta groupings are recapitulated in phylogenetic analyses of adomavirus LO8 (Adenain)
 166 homologs (Figure 4 Figure supplement 2).



167

168 **Figure 4: Sequence similarity network (BLASTP E-value threshold $1e-9$) for S3H**
 169 **proteins from indicated virus groups.**

170 Figure supplement 1: an interactive version of the figure that can be viewed using
171 Cytoscape software <https://cytoscape.org>

172 Figure supplement 2: phylogenetic tree of LO8 proteins

173 The adomavirus LT-like proteins share a full range of familiar polyomavirus-like features,
174 including an N-terminal DnaJ domain, a potential retinoblastoma-interaction motif (LXCXE or
175 LXXLFD)(An, Saenz Robles et al. 2012, Gouw, Michael et al. 2018). Several Alpha adomavirus
176 EO1 proteins encode a C-terminal domain with predicted similarity to DNA-binding RFX-type
177 winged helices (pfam02257). The RFX-like domain is conserved at the C-terminus of S3H
178 proteins found in larger dsDNA (for example, vaccinia virus D5 YP232992), some parvoviruses
179 (for example, bovine parvovirus NS1 NP_041402), and xenomaviruses. HHpred analyses
180 indicate that, like other small DNA tumor virus replicases, both classes of adomavirus S3H
181 proteins encode a central nicking endonuclease-like origin binding domain (Hickman, Ronning
182 et al. 2002, Iyer, Koonin et al. 2005, Koonin, Dolja et al. 2015, Kazlauskas, Varsani et al. 2019).

183 **Bioinformatic prediction of adomavirus virion proteins**

184 To determine whether predicted adomavirus LO proteins are expressed from spliced or unspliced
185 ORFs, RNAseq data published by Wen and colleagues (Wen, Chen et al. 2015) were analyzed to
186 determine the splicing patterns of marbled eel adomavirus transcripts. Splice acceptors
187 immediately upstream of the inferred ATG initiator codons of LO4, LO5, LO6, and LO7
188 proteins were extensively utilized (Figure 5 Figure supplement 5). Messenger RNAs encoding
189 the adenovirus late genes carry a tripartite leader (TPL) that has been shown to enhance
190 translation late in the adenovirus life cycle (Logan and Shenk 1984). A similar three-exon leader
191 sequence was detected upstream of the marbled eel adomavirus LO genes (Figure 1).

192 HHpred searches were performed to detect remote similarities between the predicted structures
193 of adomavirus proteins and known protein structures. Adomavirus LO4 proteins have a predicted
194 C-terminal trimeric coiled-coil domain. This relatively generic predicted fold gives a large and
195 diverse range of hits in HHpred searches, including the coiled-coil domains of various viral fiber
196 proteins (for example, avian reovirus σ C, 97%). Negative-stain EM images indicate that
197 adomavirus virions do not have a vertex fiber (Mizutani, Sayama et al. 2011, Wen, Chen et al.
198 2015, Dill, Camus et al. 2018). Intriguingly, LO4 proteins yielded low probability (~50%)
199 HHpred hits for adenovirus pIX, a trimeric coiled coil protein that serves as a “cement” that
200 smooths the triangular facets of the adenovirus virion. The hypothesis that LO4 is a pIX homolog
201 could hypothetically account for the smooth appearance of adomavirus virion facets in negative-
202 stain EM.

203 A C-terminal segment of some LO5 sequences, as well as alignments of multiple LO5
204 sequences, yielded moderate (~60% probability) HHpred hits for CvsA1_340L protein (single-
205 jellyroll vertex penton) of *Paramecium bursaria* chlorella virus 1 (PDB:6NCL_a6). A screen
206 shot of a typical HHpred result is shown in Figure 2 Figure supplement 2.

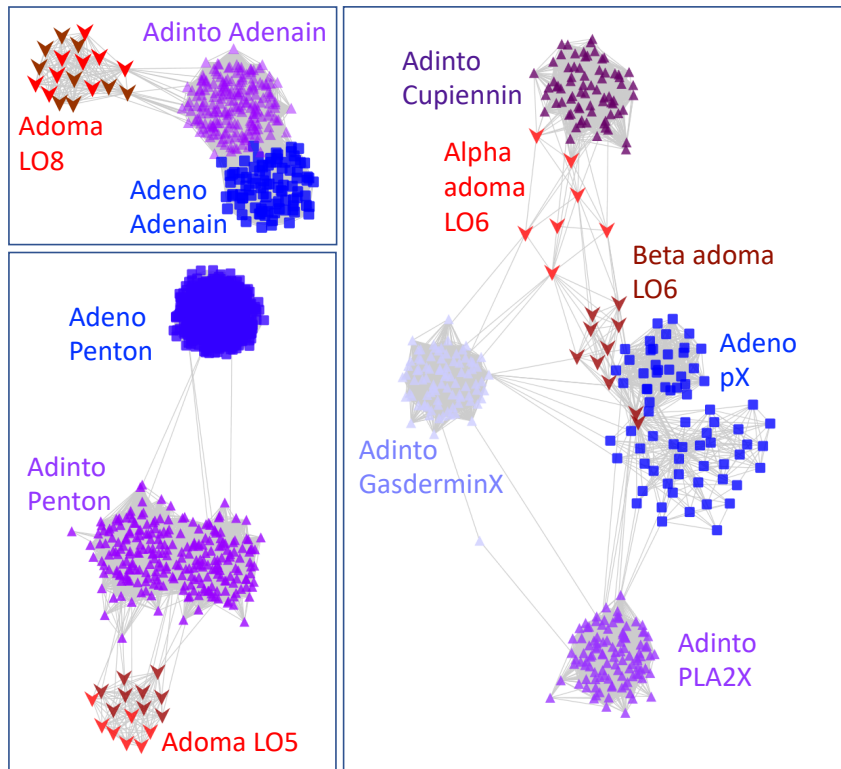
207 Alignments of LO6 ORFs show high-probability (95%) HHpred hits for a 37 amino acid
208 hydrophobic segment of adenovirus pX, a minor virion core protein that is thought to participate
209 in condensation of the viral chromatin (Nemerow, Stewart et al. 2012). LO6 alignments also
210 showed moderate probability hits (Figure 2 Figure supplement 2) for adenovirus pVI, which is

211 believed to play a role in destabilizing cellular membranes during the infectious entry process
212 (Moyer, Besser et al. 2015). The results suggest that LO6 might be a fused homolog of
213 adenovirus pVI and pX virion core proteins.

214 HHpred searches using LO7 sequences did not produce interpretable results, with the single
215 exception of the LO7 sequence of grenadier adomavirus, which gives a moderate-probability hit
216 for the V20 double-jellyroll hexon major capsid protein of Sputnik virophage (Figure 2 Figure
217 supplement 2).

218 In addition to offering a convenient way to summarize aggregate BLASTP interrelationships
219 (e.g., Figure 4), all-against-all sequence similarity network analysis can be a useful method for
220 discovering distant similarities between highly divergent groups of proteins (Iranzo, Krupovic et
221 al. 2017). In one noteworthy example, network analyses were recently used to detect remote
222 sequence similarities between small DNA tumor virus S3H replicases and CRESS virus
223 replicases (Kazlauskas, Varsani et al. 2019). In contrast to traditional analyses using
224 phylogenetic trees, it is possible for network analyses to detect individual pairs of sequences in
225 separate clusters that both happen to have preserved the primary sequence of a common ancestor.
226 We performed low-stringency network analyses to further investigate possible remote sequence
227 similarities between adenovirus, adintovirus, and candidate adomavirus virion proteins.

228 Networks for adomavirus LO4 (inferred fiber or cement protein) and LO7 (inferred double-
229 jellyroll hexon major capsid protein) showed few or no connections to adenovirus or adintovirus
230 virion protein sequences, even at a BLASTP E-value threshold of $1e-1$. In contrast, LO8
231 (adenain) proteins yielded informative networks at E-value thresholds of $1e-5$ (Figure 5). At less
232 stringent E-value thresholds ($1e-2$) similarities between adomavirus LO5 (inferred single-
233 jellyroll vertex penton) and inferred adintovirus penton protein sequences emerged. PSI-BLAST
234 searches using LO5 alignments confirmed the apparent sequence similarities (E-values $\sim 1e-6$) to
235 predicted adintovirus penton proteins found in arthropod and coral datasets (e.g., GBM63801
236 EFA12278 LSMT01002030). Although adenovirus pVI did not cluster with LO6 (inferred virion
237 core protein) or proposed adintovirus virion core proteins (Cupiennin, GasderminX, PLA2X) at
238 an E-value threshold of $1e-2$, Alpha adomavirus LO6 proteins clustered with adintovirus
239 cupiennin and Beta adomavirus LO6 proteins clustered with adenovirus pX proteins.



240

241 **Figure 5: Sequence similarity network analysis of predicted minor virion proteins.** The
242 Adenain (LO8) network was constructed with a BLASTP E-value threshold of 1e-5. Penton
243 (LO5) and virion core protein (LO6) networks used a threshold of 1e-2.

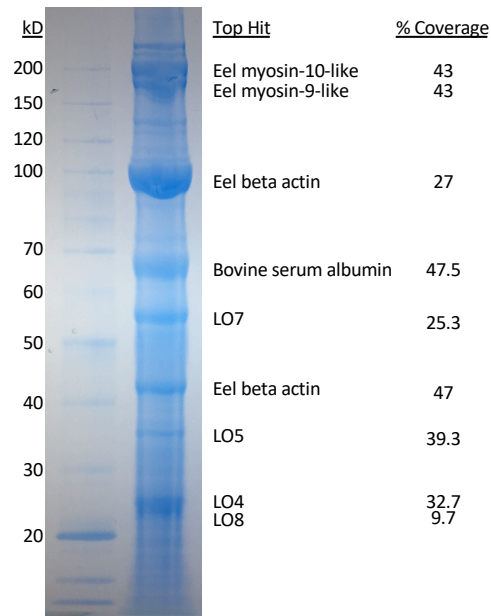
244 Figure supplement 1: an interactive version of the figure that can be viewed using Cytoscape
245 software <https://cytoscape.org>

246

247 **Experimental confirmation of predicted adomavirus virion proteins**

248 The bioinformatic results suggest that the LO4-8 operon encodes syntenic homologs of
249 adenovirus and adintovirus virion proteins. To experimentally test this prediction, marbled eel
250 adomavirus was grown in eel kidney cell culture (Wen, Chen et al. 2015) and virions were
251 purified using Optiprep gradient ultracentrifugation. Virion-enriched gradient fractions were
252 separated on SDS-PAGE gels and bands were subjected to mass spectrometric analysis (Figure
253 6). The analysis identified prominent bands in the Coomassie-stained gel as LO4, LO5, LO7, and
254 LO8. The relative intensities of bands identified as LO5 and LO7 are consistent with the
255 prediction that the two proteins constitute penton and hexon subunits, respectively. Lower
256 molecular weight bands showed hits for LO6, suggesting that this protein is present in virions in
257 an LO8 (adenain) cleaved form. LO6 proteins were found to encode potential adenain cleavage
258 motifs ((MIL)XGXG or L(LR)GG) (Ruzindana-Umunyana, Imbeault et al. 2002). A list of
259 protein modifications observed in the mass spectrometric analysis is shown in Figure 6
260 Figure supplement 1.

261



262

263 **Figure 6: SDS-PAGE analysis of marbled eel adenovirus virions purified from**
264 **infected EK-1 cells, with bands annotated by mass spectrometric analysis.** Clarified
265 lysates of infected cells were ultracentrifuged through an Optiprep gradient. Peak virion-
266 containing fractions were selected then subjected to size exclusion chromatography over
267 agarose resin. The sample was then subjected to TCA precipitation and run on an SDS-
268 PAGE gel. Thirteen gel bands were individually excised, trypsin-digested, and analyzed on
269 a Q Exactive HF Mass Spectrometer.

270 Figure supplement 1: post-translational modifications observed in mass spectrometric
271 results

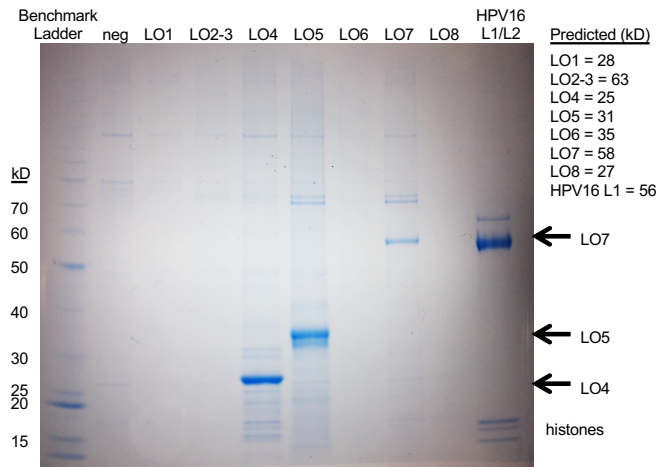
272

273 **Expression of recombinant virion proteins**

274 Adenovirus penton proteins can spontaneously assemble into 12-pentamer subviral particles that
275 may serve as decoy pseudocapsids in vivo (Vragliau, Hubner et al. 2017). Similarly,
276 recombinant polyomavirus and papillomavirus penton proteins can spontaneously assemble into
277 icosahedral virus-like particles (VLPs) that closely resemble native virions. We are not aware of
278 any reports of production of full-size (i.e., hexon+penton) adenovirus VLPs. To investigate the
279 behavior of recombinant adenovirus virion proteins, codon-modified marbled eel adenovirus
280 LO1-LO8 expression plasmids were transfected individually into human 293TT cells (Buck,
281 Pastrana et al. 2004). Optiprep ultracentrifugation was used to separate virus-like particles
282 (VLPs) from smaller solutes. A human papillomavirus type 16 (HPV16) L1/L2 expression
283 plasmid was used as a positive control for VLP formation (Buck, Thompson et al. 2005). Cells
284 transfected with adenovirus LO4, LO5, or LO7 expression constructs each produced particles
285 that migrated into the core fractions of Optiprep gradients, whereas cells transfected with LO1,

286 LO2-3, LO6, or LO8 alone did not show evidence of particle formation (Figure 7). Negative-
287 stain EM analysis showed that the LO4, LO5, and LO7 particles were irregular (Figure 7 Figure
288 supplement 1). In co-transfections of various combinations of LO genes, it was found that
289 inclusion of LO6 inhibited the formation of LO5 and LO7 particles but did not impair the
290 formation of LO4 particles (Figure 8). The fact that over-expression of LO6 can antagonize
291 particle formation supports the bioinformatic prediction that LO6 is a minor virion component
292 that directly interacts with LO5 and LO7.

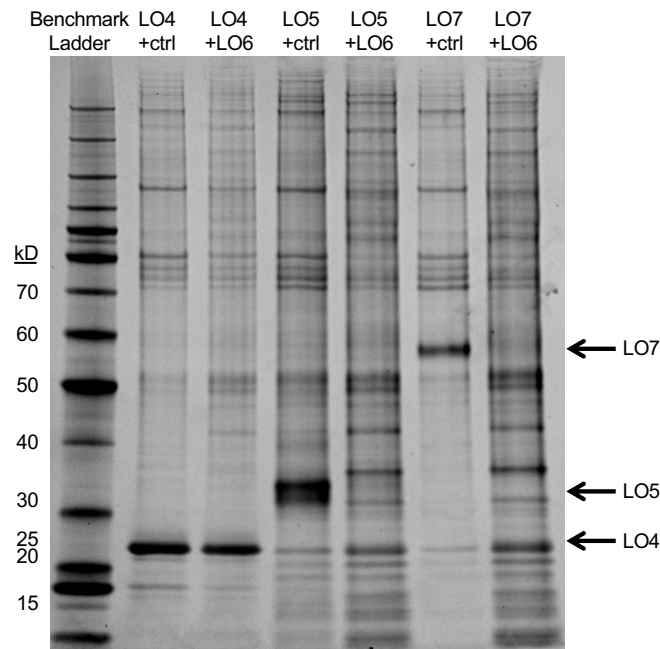
293



294

295 **Figure 7: SDS-PAGE analysis VLPs assembled in cells transfected with individual**
296 **LO expression constructs.** 293TT cells were transfected with individual codon modified
297 marbled eel LO expression plasmids indicated at the top of the image. The cells were
298 lysed, subjected to nuclease digestion and a clarifying 5000 x g spin. Soluble material
299 was ultracentrifuged through Optiprep gradients. Core gradient fractions with peak VLP
300 content were subjected to SDS-PAGE analysis.

301 Figure supplement 1: Negative-stain electron microscopy of recombinant particles.



302

303 **Figure 8: SDS-PAGE gel showing that co-expression of LO6 antagonizes LO5 and**
304 **LO7 (but not LO4) particle formation.** 293TT cells were transfected with the indicated
305 combination of plasmids and subjected to ultracentrifugal separation through Optiprep
306 gradients.

307

308 Individually expressed LO5 (penton) and LO7 (hexon) particle preparations showed dsDNA
309 signal in Quant-iT PicoGreen assays (Invitrogen), indicating the presence of nuclease-resistant
310 encapsidated DNA within the purified particles. Optiprep-purified particle preparations from
311 cells co-transfected with LO4, LO5, and LO7 were subjected to an additional round of nuclease
312 digestion with salt-tolerant Benzonase endonuclease (Sigma) followed by agarose gel filtration
313 to remove the nuclease and any residual digested DNA fragments. Nuclease-treated/gel filtered
314 particles typically contained roughly seven nanograms of DNA per microgram of total protein,
315 confirming the presence of nuclease-resistant nonspecific cellular DNA within the particles. The
316 observation is reminiscent of findings for recombinant papillomavirus VLPs (Buck, Thompson et
317 al. 2005).

318

319 Discussion

320 We have identified a dozen new representatives of the emerging virus family *Adomaviridae*.
321 Four of the new sequences are associated with terrestrial vertebrates, extending the known host
322 range beyond fish. Phylogenetic analyses reveal two adomavirus lineages that appear to have
323 independently co-evolved with host animals. This observation suggests that the two adomavirus
324 lineages both infected the first jawed vertebrates roughly half a billion years ago. Within both
325 adomavirus lineages, there are members associated with commercially important fish species.

326

327 Vaccine immunogens comprised of recombinant VLPs have been highly successful in humans
328 (Schiller and Lowy 2015). In particular, vaccines against HPVs have proven remarkably
329 immunogenic, even after a single dose. Our identification of adomavirus virion proteins and
330 demonstration of their ability to assemble into roughly spherical DNA-containing particles
331 should facilitate the development of recombinant subunit vaccines against these viruses, some of
332 which are known to cause severe disease in fish.

333 The adomavirus virion protein genes, penton (LO5), core (LO6), hexon (LO7), and adenain
334 (LO8), appear to be syntenic homologs of adenovirus and adintovirus virion protein genes. The
335 results also suggest that LO4 may be a homolog of adenovirus pIX, a trimeric coiled coil protein
336 that cements the facets of the adenovirus virion. At a primary sequence level, adomavirus virion
337 proteins more closely resemble adintovirus virion proteins, rather than adenovirus virion proteins
338 (Figure 5). These results tie the *Adomaviridae* into a broad consortium of eukaryotic virus
339 families (Koonin, Krupovic et al. 2015).

340 In unicellular eukaryotes, non-enveloped midsize (10-50 kb) dsDNA viruses have been shown to
341 have a remarkable degree of genetic modularity (Koonin, Dolja et al. 2015, Yutin, Shevchenko et
342 al. 2015) <https://www.biorxiv.org/content/10.1101/697771v3>. The pairing of related virion
343 proteins in adenoviruses, adintoviruses, and adomaviruses with entirely different classes of DNA
344 replicase genes thus has ample precedence in non-animal eukaryotes. It will be important to
345 apply emerging higher-throughput search algorithms, such as Mash Screen (Ondov, Starrett et al.
346 2019) and Cenote-Taker (Tisza, Pastrana et al. 2019), to exhaustively search for each of the
347 overlapping hallmark genes of this virus supergroup in genomic, transcriptomic, and
348 metagenomic surveys, particularly datasets for terrestrial vertebrates.

349

350 **Materials and Methods**

351 **Sample Collection and cell culture**

352 A red discus cichlid (*Symphysodon discus*) was purchased at a pet shop in Gainesville, Florida.
353 The fish was moribund and showed erythematous skin lesions. Propagation of the discus
354 adomavirus in cell culture was attempted by overlaying skin tissue homogenates on Grunt Fin
355 (GF) and Epithelioma Papulosum Cyprini cell lines (ATCC). Neither cytopathic effects nor
356 qPCR-based detection of viral replication were observed during two blind passages of 14 days
357 each.

358 Dr. Chiu-Ming Wen generously provided EK-1 cells (a Japanese eel kidney line) infected with
359 the Taiwanese marbled eel adomavirus (Wen, Chen et al. 2015). The virus was propagated by
360 inoculation of supernatants from the infected culture into uninfected EK-1 cells cultured at room
361 temperature in DMEM with 10 % fetal calf serum. Human embryonic kidney-derived 293TT
362 cells were cultured as previously described (Buck, Pastrana et al. 2004).

363 **Viral genome sequencing**

364 For the discus adenovirus, total DNA was extracted from a skin lesion and subjected to deep
365 sequencing. Marbled eel adenovirus virions were purified from lysates of infected EK-1 cells
366 using Optiprep gradient ultracentrifugation (Peretti, FitzGerald et al. 2015). DNA extracted from
367 Optiprep gradient fractions was subjected to rolling circle amplification (RCA, TempliPhi, GE
368 Health Sciences). The marbled eel adenovirus RCA products and discus total DNA were
369 prepared with a Nextera XT DNA Sample Prep kit and sequenced using the MiSeq (Illumina)
370 sequencing system with 2×250 bp paired-end sequencing reagents. In addition, the marbled eel
371 adenovirus RCA product was digested with *AclI* and *EcoRI* restriction enzymes and the
372 resulting early and late halves of the viral genome were cloned separately into the *AclI* and
373 *EcoRI* restriction sites of pAsylum+. The sequence of the cloned genome was verified by a
374 combination of MiSeq and Sanger sequencing. The clones are available upon request.

375 For the arowana adenovirus, overlapping PCR primers were designed based on WGS accession
376 numbers LGSE01029406, LGSE01031009, LGSE01028643, LGSE01028176, and
377 LGSE01030049 (Bian, Hu et al. 2016). PCR products were subjected to primer-walking Sanger
378 sequencing.

379 **Discovery of viral sequences in NCBI databases**

380 Papillomavirus E1 sequences were downloaded from PaVE <https://pave.niaid.nih.gov> (Van
381 Doorslaer, Li et al. 2017). Polyomavirus LT sequences were downloaded from PyVE
382 <https://ccrod.cancer.gov/confluence/display/LCOTF/Polyomavirus> (Buck, Van Doorslaer et al.
383 2016). Parvovirus NS1 proteins and S3H proteins of CRESS viruses and virophage-like viruses
384 were compiled from multiple databases, including RefSeq, WGS, and TSA, using TBLASTN
385 searches. Adenovirus, virophage, and bacteriophage PolB sequences were downloaded from
386 GenBank nr using DELTA-BLAST searches (Boratyn, Schaffer et al. 2012) with Alpha or Beta
387 adintovirus PolB proteins as bait.

388 SRA datasets for fish, amphibians, and reptiles were searched using DIAMOND (Buchfink, Xie
389 et al. 2015) or NCBI SRA Toolkit (<http://www.ncbi.nlm.nih.gov/books/NBK158900/>) in
390 TBLASTN mode using adenovirus protein sequences as the subject database or query,
391 respectively. Reads with similarity to the baits were collected and subjected to BLASTX
392 searches against a custom library of viral proteins representing adenoviruses and other small
393 DNA tumor viruses. SRA datasets of interest were subjected to de novo assembly using the
394 SPAdes suite (Bankevich, Nurk et al. 2012, Nurk, Meleshko et al. 2017) or Megahit (Li, Liu et
395 al. 2015, Li, Luo et al. 2016). Contigs encoding virus-like proteins were identified by TBLASTN
396 searches against adenovirus protein sequences using Bowtie (Langmead and Salzberg 2012).
397 The candidate contigs were validated using the CLC Genomics Workbench 12 align to reference
398 function.

399 Predicted protein sequences were automatically extracted from contigs of interest using getorf
400 (<http://bioinfo.nhri.org.tw/cgi-bin/emboss/getorf>) (Rice, Longden et al. 2000). Sequences were
401 clustered using EFI-EST (<https://efi.igb.illinois.edu/efi-est/>) (Gerlt, Bouvier et al. 2015, Zallot,
402 Oberg et al. 2018) and displayed using Cytoscape v3.7.1 (Shannon, Markiel et al. 2003).
403 Multiple sequence alignments were constructed using MAFFT
404 (<https://toolkit.tuebingen.mpg.de/#/tools/mafft>) (Kuraku, Zmasek et al. 2013, Katoh, Rozewicki

405 et al. 2019). Individual or aligned protein sequences were subjected to HHpred searches
406 (<https://toolkit.tuebingen.mpg.de/#/tools/hhpred>)(Hildebrand, Remmert et al. 2009, Meier and
407 Soding 2015, Zimmermann, Stephens et al. 2017) against PDB, Pfam-A, NCBI Conserved
408 Domains, and PRK databases.

409 Contigs were annotated using Cenote-Taker (Tisza, Pastrana et al. 2019) with an iteratively
410 refined library of conserved adintovirus protein sequences. Maps were drawn using MacVector
411 17. Phylogenetic analyses were performed using Phylogeny.fr with default settings (Dereeper,
412 Guignon et al. 2008).

413 **Marbled eel adenovirus transcript analysis, late ORF expression, and virion purification**

414 RNAseq reads reported by Wen et al (Wen, Chen et al. 2015) were aligned to the marbled eel
415 adenovirus genome using HISAT2 version 2.0.5 (Kim, Langmead et al. 2015) with the
416 following options: "--rna-strandness FR --dta --no-mixed --no-discordant". Integrated Genome
417 Viewer (IGV) version 2.4.9 (Robinson, Thorvaldsdottir et al. 2017) was used to determine splice
418 junctions and their depth of coverage. Additional validation was performed by visual inspection
419 using CLC Genomics Workbench 12.

420 Codon-modified expression constructs encoding the marbled eel adenovirus LO1-LO8 proteins
421 were designed according to a modified version of a previously reported algorithm
422 (https://github.com/BUCK-LCO-NCI/Codmod_as_different_as_possible)(Pastrana, Buck et al.
423 2004). 293TT cells were transfected with LO expression constructs for roughly 48 hours. Cells
424 were lysed in a small volume of PBS with 0.5% Triton X-100 or Brij-58 and Benzonase
425 Dnase/Rnase (Sigma)(Buck and Thompson 2007). After one hour of maturation at neutral pH,
426 the lysate was clarified at 5000 x g for 10 min. The clarified lysate was loaded onto a 15-27-33-
427 39-46% Optiprep gradient in PBS with 0.8 M NaCl. Gradient fractions were collected by bottom
428 puncture of the tube and screened by PicoGreen dsDNA stain (Invitrogen), BCA, or SDS-PAGE
429 analysis. Electron microscopic analysis was performed by spotting several microliters of
430 Optiprep fraction material (or, in some instances, particles exchanged out of Optiprep using
431 agarose gel filtration) onto carbon film copper grids, followed by staining with 0.5% uranyl
432 acetate.

433

434 **Mass Spectrometry**

435 Optiprep-purified marbled eel adenovirus virions were precipitated with trichloroacetic acid. A
436 1 ml sample was treated with 100 μ l of 0.15% deoxycholic acid and incubated at room
437 temperature for 10 minutes. 100 μ l of 100% TCA was then added and the sample was vortexed
438 and incubated on ice for 30 minutes. Following the incubation, the sample was centrifuged at
439 10,000 x g for 10 minutes at 4°C. The supernatant was removed, and the remaining pellet was
440 washed with ice-cold acetone to remove residual TCA. The protein pellet was solubilized with
441 NuPAGE Sample Buffer + 5% BME (Sigma) and run on a 10-12% Bis-Tris MOPS gel
442 (Thermo). The protein bands were visualized using InstantBlue (Expedeon). Thirteen gel bands
443 were individually excised and placed into 1.5 ml Eppendorf tubes. The gel bands were sent to the
444 National Cancer Institute in Fredrick, Maryland where they were de-stained, digested with
445 trypsin, and processed on a Thermo Fisher Q Exactive HF Mass Spectrometer. Thermo Proteome
446 Discoverer 2.2 software was used for initial protein identification. The uninterpreted mass
447 spectral data were also searched against *Anguilla* proteins (Swiss-Prot and TrEMBL database

448 containing 105,268 proteins), *Bos taurus* proteins (Swiss-Prot and TrEMBL database containing
449 48,288 proteins), a common contaminants database (cRAPome), and translated marbled eel
450 adenovirus ORFs. Further analysis was conducted using Protein Metrics Biopharma software to
451 identify modifications missed in initial analyses.

452 **Ethics Statement**

453 All animal tissue samples were received as diagnostic specimens collected for pathogen testing
454 and disease investigation purposes.

455 **Data Availability**

456 GenBank accession numbers for sequences deposited in association with this study are
457 BK010891 BK010892 BK011012 BK011013 BK011014 BK011015 BK011016 BK011017
458 BK011018 BK011019 BK011020 BK011021 BK012039 BK012040 BK012041 MF946549
459 MF946550 MH282863.

460

461 **Acknowledgments**

462 The authors are indebted to Eugene Koonin and Natalya Yutin for their generous guidance and
463 for the spirited discussions that inspired us to pursue this study. We are particularly grateful to
464 them for sharing their observation that adenoviruses encode a recognizable adenin homolog
465 and their discovery of adenovirus sequences in the arowana WGS datasets. The authors are also
466 grateful to Lisa Jenkins for her extensive technical guidance on analyzing mass spectrometric
467 data. We thank Karl Munger for useful discussions, including advice about oncogene sequence
468 motifs.

469

470

471 **References**

472

- 473 An, P., M. T. Saenz Robles and J. M. Pipas (2012). "Large T antigens of polyomaviruses:
474 amazing molecular machines." *Annu Rev Microbiol* **66**: 213-236.
- 475 Bacharach, E., N. Mishra, T. Briese, M. C. Zody, J. E. Kembou Tsofack, R. Zamostiano, A.
476 Berkowitz, J. Ng, A. Nitido, A. Corvelo, N. C. Toussaint, S. C. Abel Nielsen, M. Hornig, J. Del
477 Pozo, T. Bloom, H. Ferguson, A. Eldar and W. I. Lipkin (2016). "Characterization of a Novel
478 Orthomyxo-like Virus Causing Mass Die-Offs of Tilapia." *mBio* **7**(2): e00431-00416.
- 479 Bankevich, A., S. Nurk, D. Antipov, A. A. Gurevich, M. Dvorkin, A. S. Kulikov, V. M. Lesin, S.
480 I. Nikolenko, S. Pham, A. D. Prjibelski, A. V. Pyshkin, A. V. Sirotkin, N. Vyahhi, G. Tesler, M.
481 A. Alekseyev and P. A. Pevzner (2012). "SPAdes: a new genome assembly algorithm and its
482 applications to single-cell sequencing." *J Comput Biol* **19**(5): 455-477.
- 483 Belton, B., D. Little and S. Bush. (2018). "Let them eat carp: Fish farms are helping to fight
484 hunger." from [https://theconversation.com/let-them-eat-carp-fish-farms-are-helping-to-fight-](https://theconversation.com/let-them-eat-carp-fish-farms-are-helping-to-fight-hunger-90421)
485 [hunger-90421](https://theconversation.com/let-them-eat-carp-fish-farms-are-helping-to-fight-hunger-90421).
- 486 Bian, C., Y. Hu, V. Ravi, I. S. Kuznetsova, X. Shen, X. Mu, Y. Sun, X. You, J. Li, X. Li, Y. Qiu,
487 B. H. Tay, N. M. Thevasagayam, A. S. Komissarov, V. Trifonov, M. Kabilov, A. Tupikin, J.

488 Luo, Y. Liu, H. Song, C. Liu, X. Wang, D. Gu, Y. Yang, W. Li, G. Polgar, G. Fan, P. Zeng, H.
489 Zhang, Z. Xiong, Z. Tang, C. Peng, Z. Ruan, H. Yu, J. Chen, M. Fan, Y. Huang, M. Wang, X.
490 Zhao, G. Hu, H. Yang, J. Wang, J. Wang, X. Xu, L. Song, G. Xu, P. Xu, J. Xu, S. J. O'Brien, L.
491 Urban, B. Venkatesh and Q. Shi (2016). "The Asian arowana (*Scleropages formosus*) genome
492 provides new insights into the evolution of an early lineage of teleosts." *Sci Rep* **6**: 24501.
493 Boratyn, G. M., A. A. Schaffer, R. Agarwala, S. F. Altschul, D. J. Lipman and T. L. Madden
494 (2012). "Domain enhanced lookup time accelerated BLAST." *Biol Direct* **7**: 12.
495 Buchfink, B., C. Xie and D. H. Huson (2015). "Fast and sensitive protein alignment using
496 DIAMOND." *Nat Methods* **12**(1): 59-60.
497 Buck, C. B., D. V. Pastrana, D. R. Lowy and J. T. Schiller (2004). "Efficient intracellular
498 assembly of papillomaviral vectors." *J Virol* **78**(2): 751-757.
499 Buck, C. B. and C. D. Thompson (2007). "Production of papillomavirus-based gene transfer
500 vectors." *Curr Protoc Cell Biol* **Chapter 26**: Unit 26.21.
501 Buck, C. B., C. D. Thompson, Y. Y. Pang, D. R. Lowy and J. T. Schiller (2005). "Maturation of
502 papillomavirus capsids." *J Virol* **79**(5): 2839-2846.
503 Buck, C. B., K. Van Doorslaer, A. Peretti, E. M. Geoghegan, M. J. Tisza, P. An, J. P. Katz, J. M.
504 Pipas, A. A. McBride, A. C. Camus, A. J. McDermott, J. A. Dill, E. Delwart, T. F. Ng, K.
505 Farkas, C. Austin, S. Kraberger, W. Davison, D. V. Pastrana and A. Varsani (2016). "The
506 Ancient Evolutionary History of Polyomaviruses." *PLoS Pathog* **12**(4): e1005574.
507 de Souza, R. F., L. M. Iyer and L. Aravind (2010). "Diversity and evolution of chromatin
508 proteins encoded by DNA viruses." *Biochim Biophys Acta* **1799**(3-4): 302-318.
509 Dereeper, A., V. Guignon, G. Blanc, S. Audic, S. Buffet, F. Chevenet, J. F. Dufayard, S.
510 Guindon, V. Lefort, M. Lescot, J. M. Claverie and O. Gascuel (2008). "Phylogeny.fr: robust
511 phylogenetic analysis for the non-specialist." *Nucleic Acids Res* **36**(Web Server issue): W465-
512 469.
513 Dill, J. A., A. C. Camus, J. H. Leary and T. F. F. Ng (2018). "Microscopic and Molecular
514 Evidence of the First Elasmobranch Adomavirus, the Cause of Skin Disease in a Giant
515 Guitarfish, *Rhynchobatus djiddensis*." *MBio* **9**(3).
516 Gerlt, J. A., J. T. Bouvier, D. B. Davidson, H. J. Imker, B. Sadkhin, D. R. Slater and K. L.
517 Whalen (2015). "Enzyme Function Initiative-Enzyme Similarity Tool (EFI-EST): A web tool for
518 generating protein sequence similarity networks." *Biochim Biophys Acta* **1854**(8): 1019-1037.
519 Gouw, M., S. Michael, H. Samano-Sanchez, M. Kumar, A. Zeke, B. Lang, B. Bely, L. B.
520 Chemes, N. E. Davey, Z. Deng, F. Diella, C. M. Gurth, A. K. Huber, S. Kleinsorg, L. S.
521 Schlegel, N. Palopoli, K. V. Roey, B. Altenberg, A. Remenyi, H. Dinkel and T. J. Gibson (2018).
522 "The eukaryotic linear motif resource - 2018 update." *Nucleic Acids Res* **46**(D1): D428-D434.
523 Hickman, A. B., D. R. Ronning, R. M. Kotin and F. Dyda (2002). "Structural unity among viral
524 origin binding proteins: crystal structure of the nuclease domain of adeno-associated virus Rep."
525 *Mol Cell* **10**(2): 327-337.
526 Hildebrand, A., M. Remmert, A. Biegert and J. Soding (2009). "Fast and accurate automatic
527 structure prediction with HHpred." *Proteins* **77 Suppl 9**: 128-132.
528 Iranzo, J., M. Krupovic and E. V. Koonin (2017). "A network perspective on the virus world."
529 *Commun Integr Biol* **10**(2): e1296614.
530 Iyer, L. M., E. V. Koonin, D. D. Leipe and L. Aravind (2005). "Origin and evolution of the
531 archaeo-eukaryotic primase superfamily and related palm-domain proteins: structural insights
532 and new members." *Nucleic Acids Res* **33**(12): 3875-3896.

- 533 Katoh, K., J. Rozewicki and K. D. Yamada (2019). "MAFFT online service: multiple sequence
534 alignment, interactive sequence choice and visualization." Brief Bioinform **20**(4): 1160-1166.
- 535 Kazlauskas, D., A. Varsani, E. V. Koonin and M. Krupovic (2019). "Multiple origins of
536 prokaryotic and eukaryotic single-stranded DNA viruses from bacterial and archaeal plasmids."
537 Nat Commun **10**(1): 3425.
- 538 Kim, D., B. Langmead and S. L. Salzberg (2015). "HISAT: a fast spliced aligner with low
539 memory requirements." Nat Methods **12**(4): 357-360.
- 540 Koonin, E. V., V. V. Dolja and M. Krupovic (2015). "Origins and evolution of viruses of
541 eukaryotes: The ultimate modularity." Virology **479-480**: 2-25.
- 542 Koonin, E. V., M. Krupovic and N. Yutin (2015). "Evolution of double-stranded DNA viruses of
543 eukaryotes: from bacteriophages to transposons to giant viruses." Ann N Y Acad Sci **1341**: 10-
544 24.
- 545 Krupovic, M. and E. V. Koonin (2017). "Multiple origins of viral capsid proteins from cellular
546 ancestors." Proc Natl Acad Sci U S A **114**(12): E2401-E2410.
- 547 Kuraku, S., C. M. Zmasek, O. Nishimura and K. Katoh (2013). "aLeaves facilitates on-demand
548 exploration of metazoan gene family trees on MAFFT sequence alignment server with enhanced
549 interactivity." Nucleic Acids Res **41**(Web Server issue): W22-28.
- 550 Langmead, B. and S. L. Salzberg (2012). "Fast gapped-read alignment with Bowtie 2." Nat
551 Methods **9**(4): 357-359.
- 552 Li, D., C. M. Liu, R. Luo, K. Sadakane and T. W. Lam (2015). "MEGAHIT: an ultra-fast single-
553 node solution for large and complex metagenomics assembly via succinct de Bruijn graph."
554 Bioinformatics **31**(10): 1674-1676.
- 555 Li, D., R. Luo, C. M. Liu, C. M. Leung, H. F. Ting, K. Sadakane, H. Yamashita and T. W. Lam
556 (2016). "MEGAHIT v1.0: A fast and scalable metagenome assembler driven by advanced
557 methodologies and community practices." Methods **102**: 3-11.
- 558 Logan, J. and T. Shenk (1984). "Adenovirus tripartite leader sequence enhances translation of
559 mRNAs late after infection." Proc Natl Acad Sci U S A **81**(12): 3655-3659.
- 560 Meier, A. and J. Soding (2015). "Automatic Prediction of Protein 3D Structures by Probabilistic
561 Multi-template Homology Modeling." PLoS Comput Biol **11**(10): e1004343.
- 562 Mizutani, T., Y. Sayama, A. Nakanishi, H. Ochiai, K. Sakai, K. Wakabayashi, N. Tanaka, E.
563 Miura, M. Oba, I. Kurane, M. Saijo, S. Morikawa and S. Ono (2011). "Novel DNA virus isolated
564 from samples showing endothelial cell necrosis in the Japanese eel, *Anguilla japonica*." Virology
565 **412**(1): 179-187.
- 566 Moyer, C. L., E. S. Besser and G. R. Nemerow (2015). "A Single Maturation Cleavage Site in
567 Adenovirus Impacts Cell Entry and Capsid Assembly." J Virol **90**(1): 521-532.
- 568 Nemerow, G. R., P. L. Stewart and V. S. Reddy (2012). "Structure of human adenovirus." Curr
569 Opin Virol **2**(2): 115-121.
- 570 Nurk, S., D. Meleshko, A. Korobeynikov and P. A. Pevzner (2017). "metaSPAdes: a new
571 versatile metagenomic assembler." Genome Res **27**(5): 824-834.
- 572 Okazaki, S., S. Yasumoto, S. Koyama, S. Tsuchiaka, Y. Naoi, T. Omatsu, S. Ono and T.
573 Mizutani (2016). "Detection of Japanese eel endothelial cells-infecting virus in *Anguilla japonica*
574 elvers." J Vet Med Sci **78**(4): 705-707.
- 575 Ondov, B. D., G. J. Starrett, A. Sappington, A. Kostic, S. Koren, C. B. Buck and A. M. Phillippy
576 (2019). "Mash Screen: high-throughput sequence containment estimation for genome discovery."
577 Genome Biol **20**(1): 232.

578 Pastrana, D. V., C. B. Buck, Y. Y. Pang, C. D. Thompson, P. E. Castle, P. C. FitzGerald, S.
579 Kruger Kjaer, D. R. Lowy and J. T. Schiller (2004). "Reactivity of human sera in a sensitive,
580 high-throughput pseudovirus-based papillomavirus neutralization assay for HPV16 and HPV18."
581 Virology **321**(2): 205-216.
582 Peretti, A., P. C. FitzGerald, V. Bliskovsky, C. B. Buck and D. V. Pastrana (2015). "Hamburger
583 polyomaviruses." J Gen Virol **96**(Pt 4): 833-839.
584 Pipas, J. M. (2019). "DNA Tumor Viruses and Their Contributions to Molecular Biology." J
585 Virol **93**(9).
586 Rice, P., I. Longden and A. Bleasby (2000). "EMBOSS: the European Molecular Biology Open
587 Software Suite." Trends Genet **16**(6): 276-277.
588 Robinson, J. T., H. Thorvaldsdottir, A. M. Wenger, A. Zehir and J. P. Mesirov (2017). "Variant
589 Review with the Integrative Genomics Viewer." Cancer Res **77**(21): e31-e34.
590 Ruzindana-Umunyana, A., L. Imbeault and J. M. Weber (2002). "Substrate specificity of
591 adenovirus protease." Virus Res **89**(1): 41-52.
592 Schiller, J. T. and D. R. Lowy (2015). "Raising Expectations For Subunit Vaccine." J Infect Dis
593 **211**(9): 1373-1375.
594 Shannon, P., A. Markiel, O. Ozier, N. S. Baliga, J. T. Wang, D. Ramage, N. Amin, B.
595 Schwikowski and T. Ideker (2003). "Cytoscape: a software environment for integrated models of
596 biomolecular interaction networks." Genome Res **13**(11): 2498-2504.
597 Tisza, M. J., D. V. Pastrana, N. L. Welch, B. Stewart, A. Peretti, G. J. Starrett, Y.-Y. S. Pang, A.
598 Varsani, S. R. Krishnamurthy, P. A. Pesavento, D. H. McDermott, P. M. Murphy, J. L. Whited,
599 B. Miller, J. M. Brenchley, S. P. Rosshart, B. Rehmann, J. Doorbar, B. A. Ta'ala, O.
600 Pletnikova, J. Troncoso, S. M. Resnick, A. M. Segall and C. B. Buck (2019). "Discovery of
601 several thousand highly diverse circular DNA viruses." 555375.
602 Van Doorslaer, K., Z. Li, S. Xirasagar, P. Maes, D. Kaminsky, D. Liou, Q. Sun, R. Kaur, Y.
603 Huyen and A. A. McBride (2017). "The Papillomavirus Episteme: a major update to the
604 papillomavirus sequence database." Nucleic Acids Res **45**(D1): D499-d506.
605 Vragliau, C., J. M. Hubner, P. Beidler, S. Gil, K. Saydaminova, Z. Z. Lu, R. Yumul, H. Wang,
606 M. Richter, P. Sova, C. Drescher, P. Fender and A. Lieber (2017). "Studies on the Interaction of
607 Tumor-Derived HD5 Alpha Defensins with Adenoviruses and Implications for Oncolytic
608 Adenovirus Therapy." J Virol **91**(6).
609 Wen, C. M., M. M. Chen, C. S. Wang, P. C. Liu and F. H. Nan (2015). "Isolation of a novel
610 polyomavirus, related to Japanese eel endothelial cell-infecting virus, from marbled eels,
611 *Anguilla marmorata* (Quoy & Gaimard)." J Fish Dis.
612 Yutin, N., S. Shevchenko, V. Kapitonov, M. Krupovic and E. V. Koonin (2015). "A novel group
613 of diverse Polinton-like viruses discovered by metagenome analysis." BMC Biol **13**: 95.
614 Zallot, R., N. O. Oberg and J. A. Gerlt (2018). "'Democratized' genomic enzymology web tools
615 for functional assignment." Curr Opin Chem Biol **47**: 77-85.
616 Zimmermann, L., A. Stephens, S. Z. Nam, D. Rau, J. Kübler, M. Lozajic, F. Gabler, J. Söding,
617 A. N. Lupas and V. Alva (2017). "A Completely Reimplemented MPI Bioinformatics Toolkit
618 with a New HHpred Server at its Core." J Mol Biol **S0022-2836**(17): 30587-30589.

619